SCIPEDIA

Numerical Simulation of the Influence of Different Opening Parameters on the Flexural Performance of Fixed Open-Web Steel Beams

Qingxing Feng[1], Meizhong Qian[1], Chen Qu[1,*] and Nihong Ye[2]

[1] School of Civil Engineering and Architecture, Zhejiang University of Science and Technology, Hangzhou, 310023, China

[2] Party Building Department, Zhejiang Wuyi Zhanye Pipeline Construction and Operation Co., Ltd., Jinhua, 321200, China

INFORMATION

Keywords:
Open-web steel beam
flexural performance
opening rate
end distance
opening distribution
numerical simulation

DOI: 10.23967/j.rimni.2025.10.64829

SCIPEDIA Revista Internacional de Métodos Numéricos para Cálculo y Diseño en Ingeniería

RIMNI Revista Internacional Métodos numéricos para cálculo y diseño en ingeniería

Numerical Simulation of the Influence of Different Opening Parameters on the Flexural Performance of Fixed Open-Web Steel Beams

Qingxing Feng[1], **Meizhong Qian**[1], **Chen Qu**[1,*] **and Nihong Ye**[2]

[1]School of Civil Engineering and Architecture, Zhejiang University of Science and Technology, Hangzhou, 310023, China

[2]Party Building Department, Zhejiang Wuyi Zhanye Pipeline Construction and Operation Co., Ltd., Jinhua, 321200, China

ABSTRACT

Based on the ABAQUS finite element analysis software platform, this study investigated the effects of opening parameters, including end distance, opening rate, and opening distribution, on the flexural performance of fixed open-web steel beams. The results indicate that an open-web steel beam with fixed support exhibits a flexural shear failure mode, which initiates yielding at the hole corners in the flexural shear zone. As the load increases, the plastic zone progressively extends to the flange, ultimately forming a four-hinge plastic mechanism around the hole. Specifically, a mid-span hole reduces the flexural performance by approximately 10%, while an end hole reduces it by approximately 47%. It is recommended that mid-span openings with end distances no less than 1.75 times the beam height be prioritized in engineering design. Additionally, the flexural performance of fixed open-web steel beams decreases as the opening rate increases. Optimizing the opening geometry by reducing its length-to-height ratio under invariant opening ratio conditions provides a more than doubled flexural capacity gain, offering practical insights for beam design.

OPEN ACCESS

Received: 25/02/2025

Accepted: 24/03/2025

Published: 14/07/2025

DOI
10.23967/j.rimni.2025.10.64829

Keywords:
Open-web steel beam
flexural performance
opening rate
end distance
opening distribution
numerical simulation

1 Introduction

Open-web steel beams emerged in the 1940s and were initially utilized during World War II to reduce the costs of steel buildings [1]. Currently, they are essential in modern architecture to fulfill functional needs, such as high ceilings, large spaces, and wide spans, and they often require holes in floor beams to create open-web designs.

The mechanical properties of open-web beams are influenced by factors such as the hole type, hole-opening ratio, hole spacing, hole height ratio, and hole length-to-height ratio. Several researchers have conducted studies on this topic. Wu et al. [2] examined the impact of the span, hole-opening ratio, and hole spacing on the mechanical properties of hexagonal perforated beams and provided practical calculation formulas. Morkhade et al. [3] investigated the influence of the width of the web column between holes on the bearing capacity of open-web steel beams and summarized the influence law of hole spacing on the failure mode of open-web beams. Wang et al. [4] studied the elastic-plastic

*Correspondence: Chen Qu (quchen@zust.edu.cn).

development process of open-web beams and discovered that although increasing the section height can enhance the flexural rigidity of the component, it also reduces the shear bearing capacity, owing to the excessive hole-opening in the web plate. Al-Rifaie et al. [5] discovered that a wide opening considerably diminishes the bending performance, whereas horizontal stiffening markedly enhances the bending performance. Song [6] conducted experiments and simulation studies on the mechanical performance of large-scale nonequidistant rectangular perforated steel beams, proposed the concept of the influence area of the hole-opening, and proposed the coefficients of increased normal stress and shear stress based on existing theoretical formulas. Wang [7] and Liu [8] investigated the impact of the span-to-height, hole-height, length-to-height, and distance-to-height ratios on the mechanical properties of rectangular open-web beams and proposed improved stress formulas. Ponsorn et al. [9] discovered that broken line cutting exhibits superior performance compared to circular holes, and the optimal opening configuration is contingent upon the beam's length and service conditions. Zhu et al. [10] discovered that perforating the high-shear zone significantly compromises the strength of the structural member. Xu et al. [11–13] conducted bending performance tests on simply supported open-web steel beams with diverse hole-opening parameters and summarized the influence laws of factors, including the hole-opening ratio, hole distribution, and hole length-to-height ratio, on the bending performance of simply supported open-web steel beams. Zou et al. [14,15] and Jia et al. [16]. Performed a static loading test to compare the flexural capacities of simply supported circular beams and hexagonal beams. Their results demonstrate that circular openings exhibit superior performance relative to hexagonal openings, with flexural capacity decreasing progressively as the opening ratio increases. Wang [17] investigated the failure mechanisms of steel beams featuring rectangular openings in the web and derived a formula for calculating their plastic bearing capacity, grounded in the theory of four-axis force-bending moment plastic hinges. Luo et al. [18] concentrated on the stress distribution of simply supported open-web steel beams. They compared and analyzed the calculation results from the former Soviet Union code, the Japanese code, and the finite element software, and subsequently put forward an improved calculation for normal stress of the cross-section considering the opening parameters and load conditions. Hosseinpour et al. [19] proposed a method based on an Artificial Neural Network to predict the ultimate bending capacity of open-web steel beams. Maalek [20] deduced the formula for the shear deflection of the web between the holes and carried out experimental verification. Based on the principles of area equivalence and inertia moment equivalence. Li et al. [21] derived a practical formula for calculating the deflection of a hexagonal open-web beam with simple support. Zhou et al. [22] critically evaluated the existing methodologies for calculating flexural rigidity and proposed a practical formula for determining the equivalent flexural rigidity of open-web beams. Li [23] proposed a method for calculating the initial rotational stiffness of the end-plate connection of H-shaped column with honeycomb beam. Huang et al. [24] employed the Simpson formula to address the integral equation featuring variable moments of inertia during the solution process of the differential equation for the flexural line, thereby deriving an expression for the equivalent flexural stiffness of open-web beams. Budi et al. [25] optimized hole angle and hole distance parameters of hexagonal simply supported web-open beams by finite element analysis. Shamass et al. [26] presents a simplified mechanical model for web-post buckling failure through finite element analysis of simply supported open-pass beams with varying steel strengths. Due to the presence of open holes, the flexural performance of steel beams is diminished. Consequently, numerous scholars have dedicated their efforts to investigating methods for reinforcing hollow steel beams. For instance, installing stiffeners around open holes [27,28], utilizing high-strength steel [29], enlarging the cross-sectional dimensions [30], and employing composite structures [31] can enhance the flexural performance of open-web steel beams. Zhai [32] concluded that reinforcing the mid-span open-hole beam with a plate and the end open-hole beam with a stiffener would satisfy the engineering requirements. The mechanical

response of a beam with fixed support differs from that of a beam with simple support due to varying constraint conditions. Under identical loading conditions, the bearing capacity and stiffness of a fixed-supported beam are superior to those of a simply supported beam. Huang et al. [33] investigated the elastoplastic behavior of simply supported and fixed open-web beams, revealing that an open hole at the end is prone to shear failure. However, further research is required to determine an appropriate end distance value. Chen [34] proposed that the appropriate opening radius for a circular open-hole beam with fixed support should be between H/4 and H/3. Su et al. [35] compared the mechanical performance of the hollow beam with circular holes, hexagonal holes, and rectangular holes, and the results showed that the mechanical performance of the hexagonal holes was the best, followed by the circular holes, and the rectangular holes were the worst, which was different from the law in the case of simple supports. Zheng et al. [36] conducted static loading tests on six fixed-end open-web beams with different hole length-to-height ratios, hole-opening ratios, and hole distributions as well as summarizing the influence laws of hole-opening parameters on the bearing capacities of fixed-end open-web steel beams.

Currently, the majority of research both domestically and internationally has concentrated on simply supported open-web steel beams. However, there is a relative paucity of studies examining the mechanical behavior of fixed-end open-web steel beams. Although under identical loading conditions, the bending moment distribution in fixed-end beams is more uniform compared to simply supported beams of equal span, the shear force at sections with higher bending moments is comparatively greater. This increased shear force may result in premature failure of the beam. Consequently, it is necessary to investigate the mechanical performance of fixed-end open-web steel beams. In this study, using open-web steel beams featuring triangular chamfered holes as the research object, numerous numerical models of fixed-end open-web steel beams were established using the ABAQUS software. Considering the end distance, hole height ratio, hole length-to-height ratio, hole-opening ratio, and number of holes as variables, the degrees of reduction of each parameter on the bearing capacity and stiffness of the components were compared and analyzed. The influence laws of each factor on the bearing capacity and stiffness of the components were summarized, and suggestions for reasonable hole-opening parameters were proposed.

2 Finite Element Model Building

2.1 Model Building

In this study, the steel beam span of the model was 3 m, section size was H300 × 75 × 5 × 7 (unit: mm), steel strength grade was Q235, elastic modulus was 206 GPa, and Poisson's ratio was 0.3. The constitutive model of steel is an ideal elastic-plastic model. In ABAQUS, the web could be perforated using a "cutting" operation. Fig. 1 shows a three-dimensional finite element calculation model of an open-web steel beam.

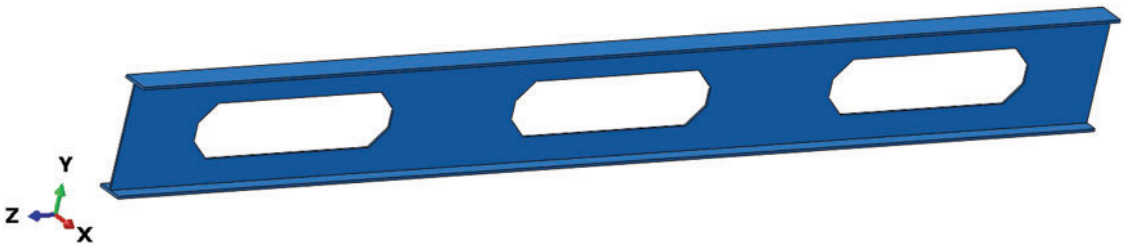

Figure 1: Three-dimensional finite element calculation model of an open-web steel beam

2.2 Mesh Dividing

Fig. 2 shows the mesh division diagram. To ensure calculation accuracy and efficiency, an 8-node hexahedral linear reduction integral element (C3D8R) with a mesh size of 5 mm was employed as the grid element type. In addition, to reflect the stress state in the direction of flange and web thickness, the number of grid division layers in the direction of web and web thickness was defined as 3 layers.

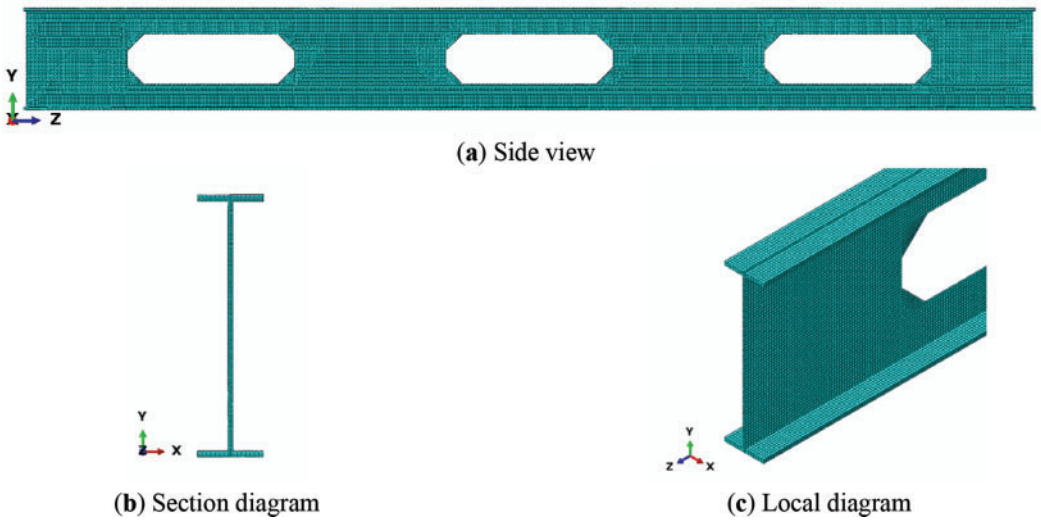

Figure 2: Mesh division

2.3 Boundary Condition and Load Settings

Finite element model was verified with the experimental results conducted by Xu et al. [11–13]. On this basis, the boundary conditions were changed to two fixed ends for analysis. The loading method adopted three-point concentrated force loading. The boundary conditions are fixed constraints at both ends. Thus, the translational constraints u_x, u_y, and u_z in three directions and rotation constraints θ_x, θ_y, and θ_z in three directions are applied at the beam ends. Here, x, y, and z correspond to the directions of the global coordinate system, indicating the directions along the beam width, height, and axis, respectively. Fig. 3 shows a schematic of the boundary conditions.

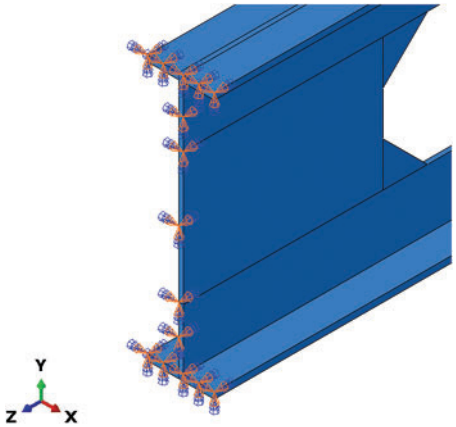

Figure 3: Boundary condition

3 Finite Element Model Parameter Analysis

3.1 Parameter and Output Data Description

3.1.1 Parameter Description

Fig. 4 shows the variables used for parameter analysis. For convenience of expression, the calculation model number is specified as "M-h_0-l_0-e-n," where "M" indicates the model, "h_0" indicates opening height, "l_0" indicates opening length, "e" indicates end distance, and "n" indicates the number of opening holes. The number of the solid web beam model is denoted by "M_0." Computational models were compared using the control variable method to maximize the consistency of the remaining variables. Only the variables under study were altered.

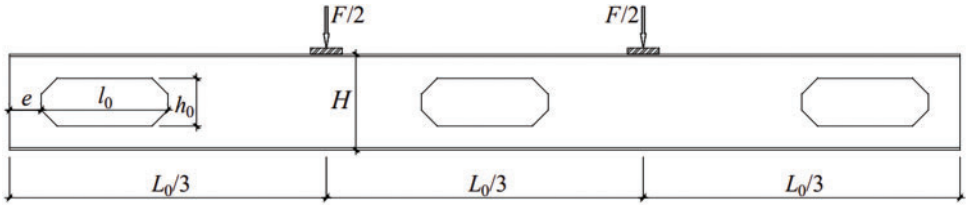

Figure 4: Variable diagram. Note: h_0/H represents the ratio of opening height to section height. l_0/h_0 represents the ratio of opening length to opening height. e/H represents the ratio of end distance to section height. The opening rate k represents the ratio of the hole area to the solid beam web area. L_0 represents the beam span

3.1.2 Output Data Description

The simulation results mainly output the load–deflection curve and stress nephogram. The ultimate load and elastic stiffness values can be obtained from the load–deflection curve as follows. The vertical coordinate corresponding to the peak point of the load–deflection curve is the ultimate load F_{max}. When the load–deflection curve remained linear, the slope was the elastic stiffness, K_e.

The simulation results were compared with the equivalent solid web beams as a reference, and the weakening degree of the flexural performance caused by the opening parameters was characterized by the reduction percentage. The reduction percentage indicates the extent of reduction in the equivalent solid web beams, owing to the opening parameters.

3.1.3 Typical Load-Deflection Curve

Fig. 5 illustrates the typical load-deflection curve of a steel beam, which can be divided into three distinct stages: the elastic stage, the plastic development stage, and the failure stage. The stress nephogram of each stage is shown in Fig. 6.

(1) Elastic stage: In the first segment of the curve, the entire component remains in an elastic state, with the load-deflection relationship being linear. The elastic stage concludes when certain fibers reach the material's yield strength. The corresponding load value is designated as the elastic limit F_e, while the associated deflection value is termed the elastic deflection Δ_e. This stage corresponds to Fig. 6a. At the end of the beam, the stress concentration at the hole angle reached the yield point first, whereas the stress at the hole angle in the mid-span remained lower. This phenomenon occurred because the beam end was primarily subjected to bending moments and shear forces, which led to significant stress concentration at the hole angle. In contrast, the

mid-span hole was mainly influenced by bending moments, resulting in a relatively lower stress level.

(2) Plastic development stage: An increasing number of fibers enter the yield phase, leading to the expansion of the plastic zone. Sections progressively transition into full-section plasticity. This stage is characterized by a distinct inflection point, defined as the yield point of the component. The corresponding load value is identified as the yield load F_y, and the associated deflection value is referred to as the yield deflection Δ_y. This stage corresponds to Fig. 6b. The angle plastic zone of the beam end hole gradually expanded to the flange, forming four plastic zones.

(3) Failure stage: Multiple plastic hinges form within the member until it transforms into a "mechanism," indicating that the member has reached its ultimate bearing capacity. The maximum load value at this stage is denoted as the ultimate load F_{max}, and the corresponding deflection value is termed the ultimate deflection Δ_{max}. This stage corresponded to Fig. 6c, where the plastic zone extended across the entire section until the structure failed.

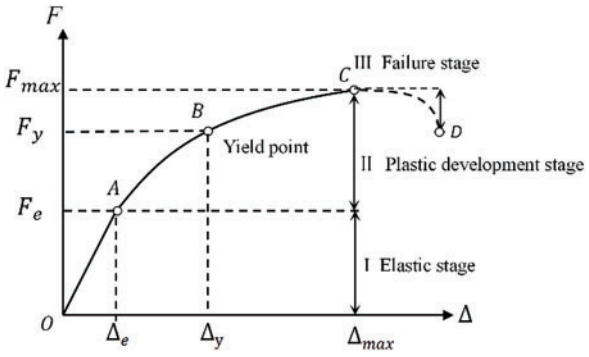

Figure 5: Typical load-deflection curve

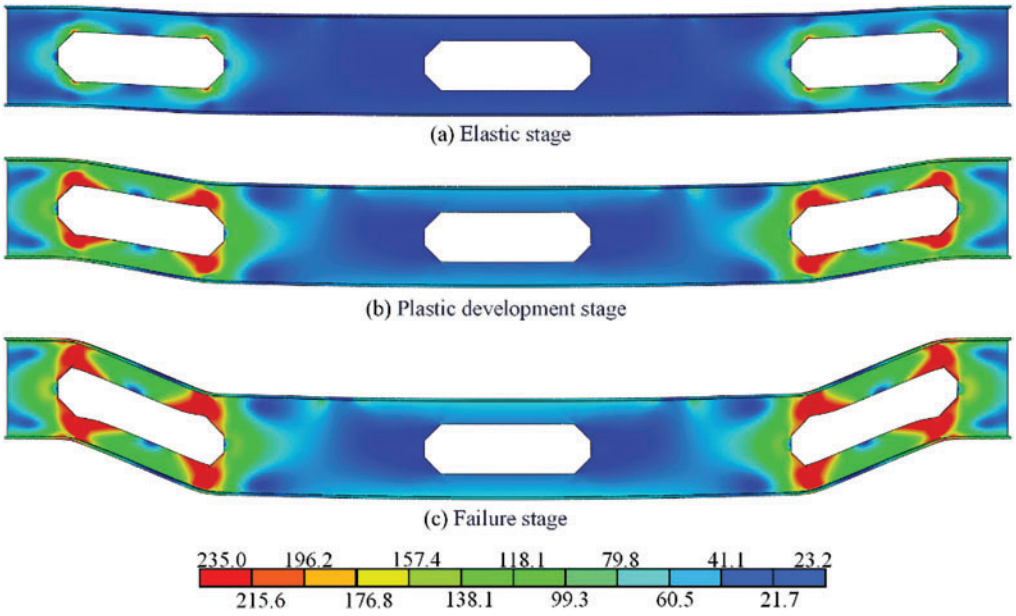

Figure 6: Stress nephogram (unit: MPa)

3.2 End Distance

To study the influences of different end distances on the flexural performance of the open-web steel beam, four-hole length-to-height ratios (1.0, 1.33, 1.67, and 2.0) were selected. The control hole height ratio was held constant at 0.5. Eleven end distances (75, 150, 225, 300, 375, 450, 525, 600, 750, 900, 1050 mm) caused e/H to change within 0.25–3.5, and a total of 45 models were established. The holes of the model with an end distance of 1050 mm were located in the middle of the span, whereas the maximum end distance was 1000 mm for those of the model with a hole length of 300 mm. These results occurred because the pure bending section area could not row three holes when the end distance was 1050 mm.

3.2.1 Stress Nephogram

Fig. 7 shows the stress nephograms of the models M-150-150-75-3, M-150-150-525-3, M-150-150-1050-3, and M_0 under the ultimate load. Variations exist in the failure modes of the steel beams with different end distances.

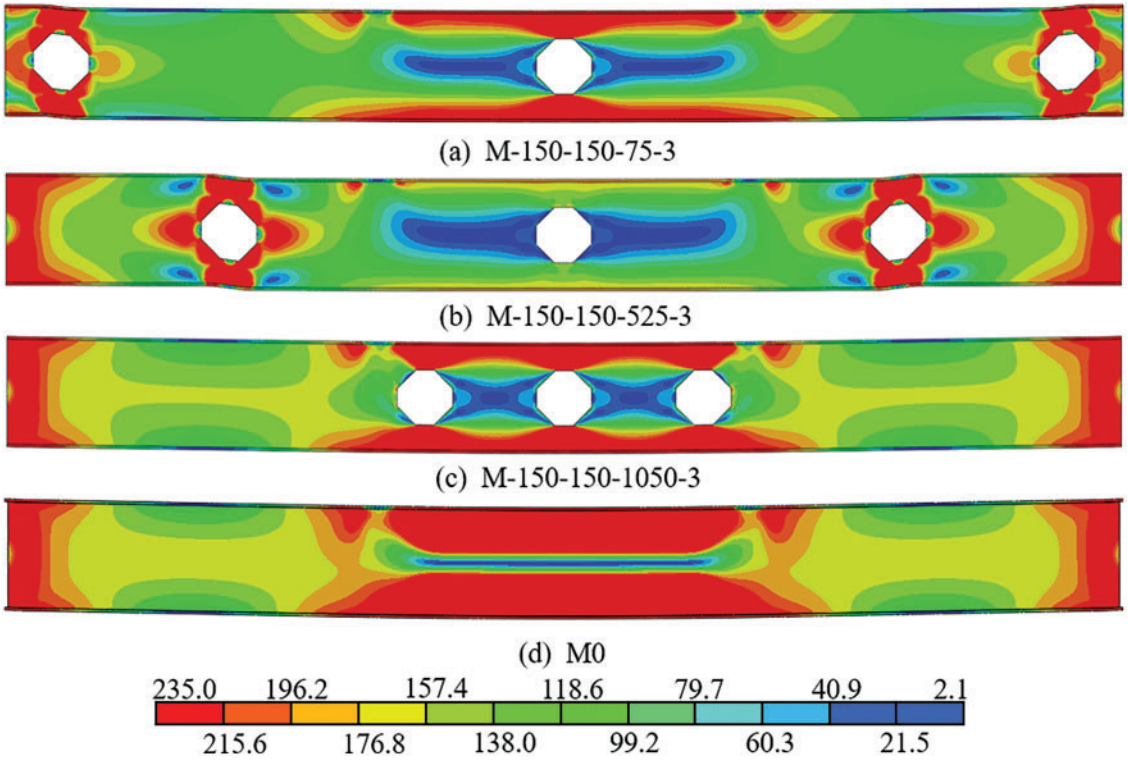

Figure 7: Stress nephogram (unit: MPa)

In Fig. 7a, for small end distances, plastic hinges initially developed around the beam-end hole, resulting in a noticeable deformation of the hole shape. Subsequently, plastic hinges formed in the mid-span region, indicating a bending–shear failure mode. This phenomenon occurred because the opening caused a reduction in the shear stiffness of the section and led to stress concentration at the hole angle, ultimately resulting in plastic hinge formation near the beam end opening.

In Fig. 7b, when larger end distances were considered, plastic hinges appeared at both the beam end and around the beam-end hole. However, no plastic hinge fracture occurred at the mid-span. The

presence of an opening weakens the shear stiffness within this section and initiates bending–shear failure primarily at the opening location, which thereby prevents further load-bearing capacity within the midspan area.

In Fig. 7c, when openings are concentrated within pure bending sections, the failure modes resemble those observed in solid web beams, where plastic hinge fractures occur at both the beam ends and mid-span regions, whereas the ultimate load is governed by the net section behavior within the mid-span area.

3.2.2 Elastic Stiffness

Fig. 8 shows the line diagram of elastic stiffness changing with end distance when the hole length-to-height ratio is 1.0–2.0. The horizontal dashed line in Fig. 8 represents the elastic stiffness of the equivalent solid web beam, and the percentage reduction represents the reduction percentage, relative to the equivalent solid web beam.

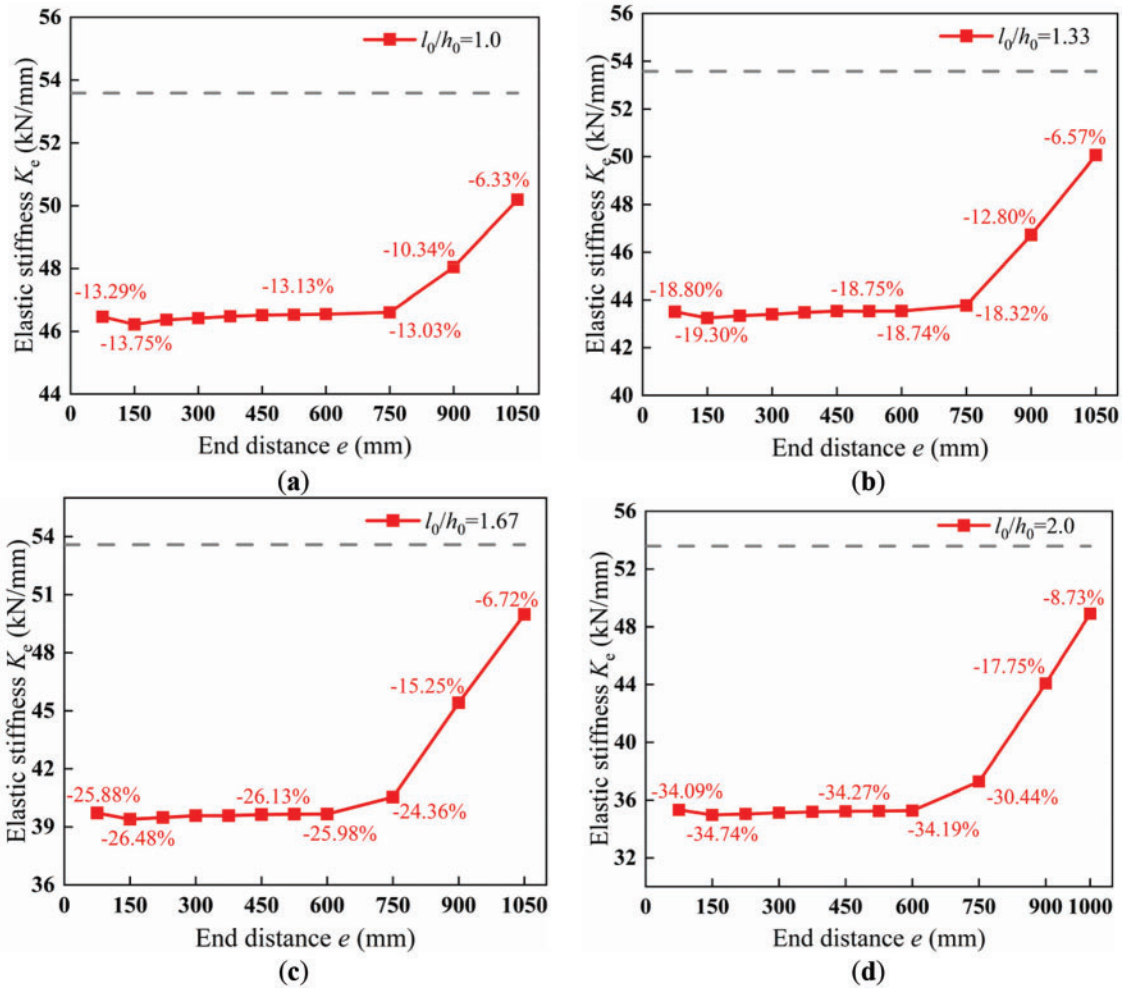

Figure 8: Elastic stiffness–end distance line graph with different length-to-height ratios. (a) $l_0 = 150$ mm, $k = 0.079$; (b) $l_0 = 200$ mm, $k = 0.105$; (c) $l_0 = 250$ mm, $k = 0.131$; (d) $l_0 = 300$ mm, $k = 0.157$

The variation trend of the elastic stiffness with the end distance remained consistent across different length-to-height ratios and exhibited a double-fold line pattern. For end distances of less than 750 mm (2.5 H), the plot of the elastic stiffness–end distance for each model approximates a straight line with a slight slope. However, a significant increase in the elastic stiffness of each model was observed when the end distance exceeded 750 mm.

When the end distance was varied by 750 mm, the reduction in the elastic stiffness remained stable, whereas the range of reduction increased with an increase in the hole length-to-height ratio. These results suggest that adjusting the end distance has a limited effect on the enhancement of the elastic stiffness of a beam with an endhole.

When the end distance exceeded 750 mm and the hole length-to-height ratio was set at 1.0, 1.33, 1.67, and 2.0, corresponding elastic stiffness reductions of 6.7%, 11.75%, 17.64%, and 21.71%, respectively, were observed, indicating a significant enhancement in elastic stiffness with an increasing end distance and an even more pronounced effect with a higher hole length-to-height ratio.

When the openings are all located at mid-span, that is, when the end distance is 1050 mm, the corresponding reduction percentages of hole length-to-height ratios of 1.0, 1.33, 1.67, and 2.0 are −6.33%, −6.57%, −6.72%, and −8.73%, respectively. These results indicate that when the openings are all located at midspan, the influence on the elastic stiffness is small, and the influence of different hole length-height ratios on the elastic stiffness is insignificant.

3.2.3 Ultimate Load

As depicted in Fig. 9, the ultimate load of components with different length-to-height ratios exhibits a similar trend with varying end distances within a range of 1.0–2.0. For end distances below 750 mm, the ultimate load-end distance relationship for each model approximates a straight line with a small slope, showing a significant maximum value at 525 mm. However, when the end distance exceeded 750 mm, there was a substantial increase in the ultimate load for each model as the end distance increased.

The degree of the reduction in the ultimate load remained stable when the end distance was varied within 750 mm. Moreover, the variation range of the degree of reduction decreased as the end distance increased. This observation suggests that changes in the end distance have a minimal effect on the ultimate bearing capacity of the member. Conversely, variations in the hole length-to-height ratio significantly affected the ultimate bearing capacities of the members. Therefore, for beams with openings at the ends, the range of increase in the ultimate load that is achievable by adjusting the end distance is limited. Instead, the opening rate should be adjusted.

When the end distance exceeded 750 mm, the ultimate load increased significantly. The increments in the percentage reduction of the ultimate load corresponding to the hole length-to-height ratios of 1.0, 1.33, 1.67, and 2.0, are 13.63%, 24.63%, 33.61%, and 38.48%, respectively. These findings indicate that a larger hole length-to-height ratio results in a more pronounced increase in the ultimate load upon adjusting the end distance.

When the openings are all located in the mid-span position, that is, when the end distance is 1050 mm, the reduction percentage corresponding to the hole length-to-height ratio of 1.0–2.0 is approximately −4.12%. These results indicate that when the openings are all located in the midspan position, they have little effect on the ultimate load, and the change in the hole length-to-height ratio has little effect on the flexural performance of the open-web steel beam. Comparing Figs. 8 and 9

shows that the impact of the openings on the ultimate load was slightly greater than that on elastic stiffness.

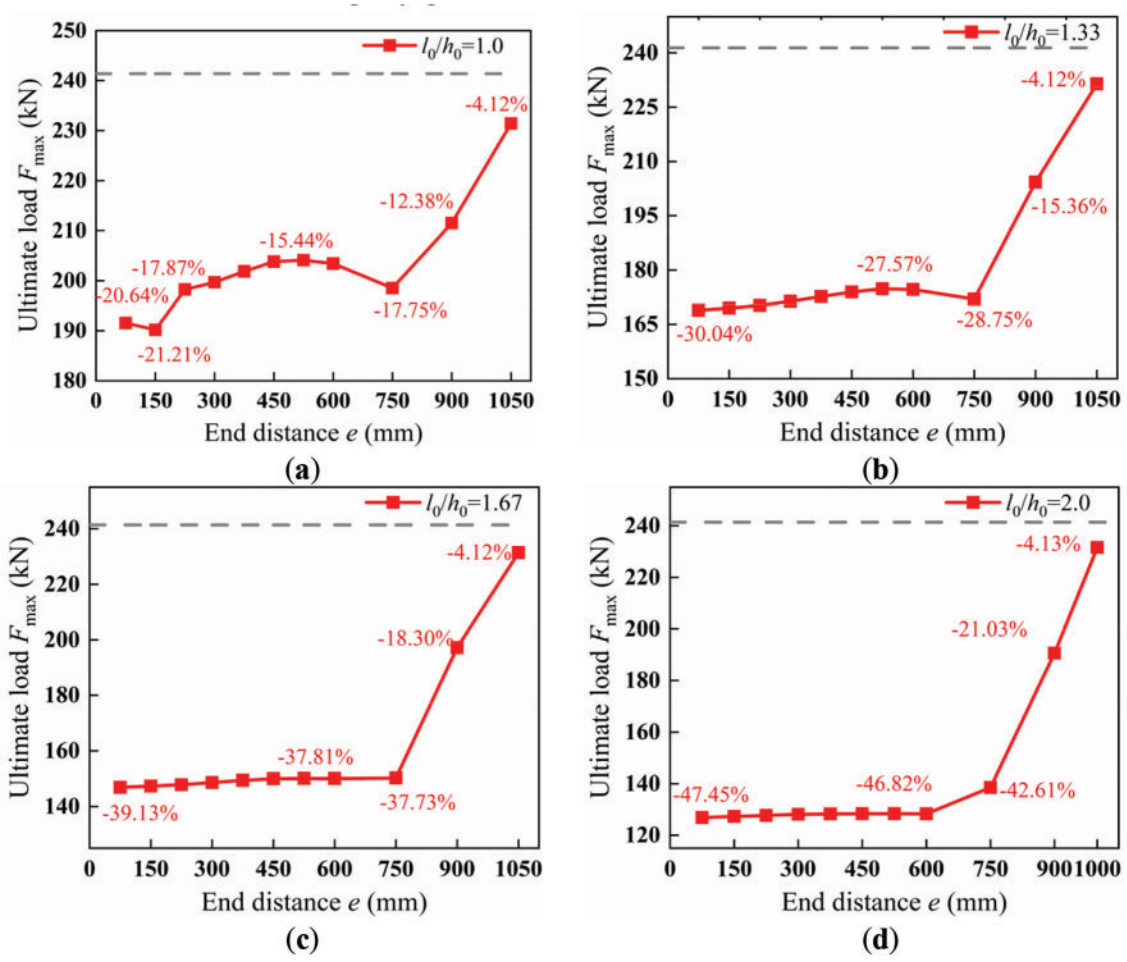

Figure 9: Ultimate load-end distance line graph with different length-height ratio. (a) $l_0 = 150$ mm, $k = 0.079$; (b) $l_0 = 200$ mm, $k = 0.105$; (c) $l_0 = 250$ mm, $k = 0.131$; (d) $l_0 = 300$ mm, $k = 0.157$

Variations in the end distance and the length-to-height ratio of the hole influence both the bearing capacity and stiffness of the open-web steel beam. The presence of an opening at the end of the beam led to a greater reduction in the bearing capacity and stiffness, which correlated with the length-to-height ratio of the hole. When the openings were located within midspan, the flexural behavior of the open-web steel beam closely approximated that of a solid girder.

Based on the simulation results presented in this section, Fig. 10 illustrates the relationship between the end distance and flexural resistance of the open-web steel beam. For end distances less than 2.5 H, the changes in the elastic stiffness and ultimate load are relatively gradual; however, once the end distance exceeds 2.5 H, further increases have a pronounced impact on both the bearing capacity and stiffness.

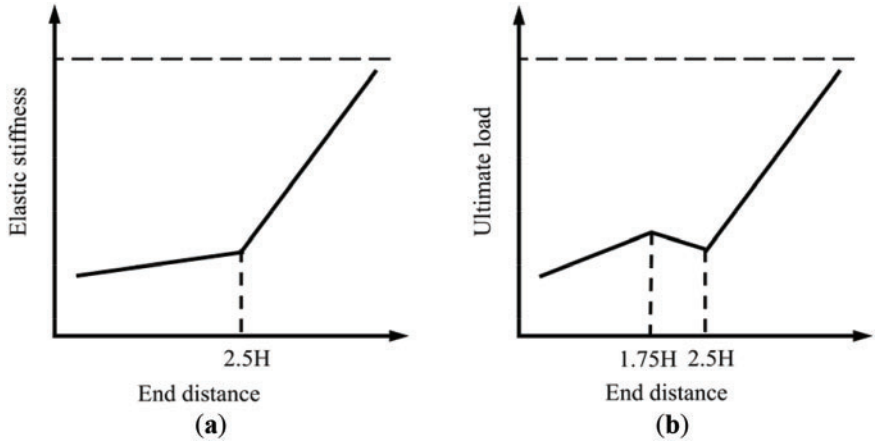

Figure 10: Relation diagram of elastic stiffness, ultimate load, and end distance. (a) Diagram of the relationship between elastic stiffness and end distance; (b) Diagram of the relationship between ultimate load and end distance

Fig. 10b illustrates the relationship between the variations in the end distance and the ultimate load for an open-web steel beam. At an approximate end distance of 1.75 H, the effect of opening at this location on the flexural bearing capacity was minimized. Therefore, unless specific requirements dictate otherwise regarding opening placement, it is advisable to position openings centrally within the span or at an end-distance of approximately 1.75 H to mitigate their impact on the flexural performance of each member.

3.3 Opening Rate

To investigate the influence of the opening rate change caused by altering the opening length and opening height on the bearing capacity and stiffness, the fixed end distance was set to 300 mm, and five opening heights (100, 120, 150, 180, and 210 mm) as well as six opening lengths (150, 200, 300, 400, 500, and 600 mm) were considered, comprising a total of 30 models.

3.3.1 Opening Length

Fig. 11 shows the broken line graph of the elastic stiffness opening length for models with different opening heights. As the opening length increases, the elastic stiffness exhibits a monotonically decreasing trend. The opening length is closely related to the weakening of the elastic stiffness of the member, and a larger opening length implies a smaller stiffness of the member. The broken line graph shows that for every 100 mm increase in the average opening length, the elastic stiffness reduction degrees corresponding to the opening heights of 100, 120, 150, 180, and 210 mm increase by approximately 10.53%, 11.54%, 13.01%, 14.15%, and 14.74%, respectively. These findings indicate that a higher opening height results in a greater reduction rate of elastic stiffness when the same opening length is changed.

In Fig. 11a, the reduction percentage of the elastic stiffness of the model with a hole height of 100 mm and hole length of 600 mm is −60.76%, indicating that even if the hole height is small, the elastic stiffness is greatly weakened when the hole length is large. In Fig. 11e, the reduction percentage of the elastic stiffness of the model with a hole height of 210 mm and hole length of 120 mm is −21.03%, indicating that even if the hole height is small, the elastic stiffness is significantly weakened when the hole height is large.

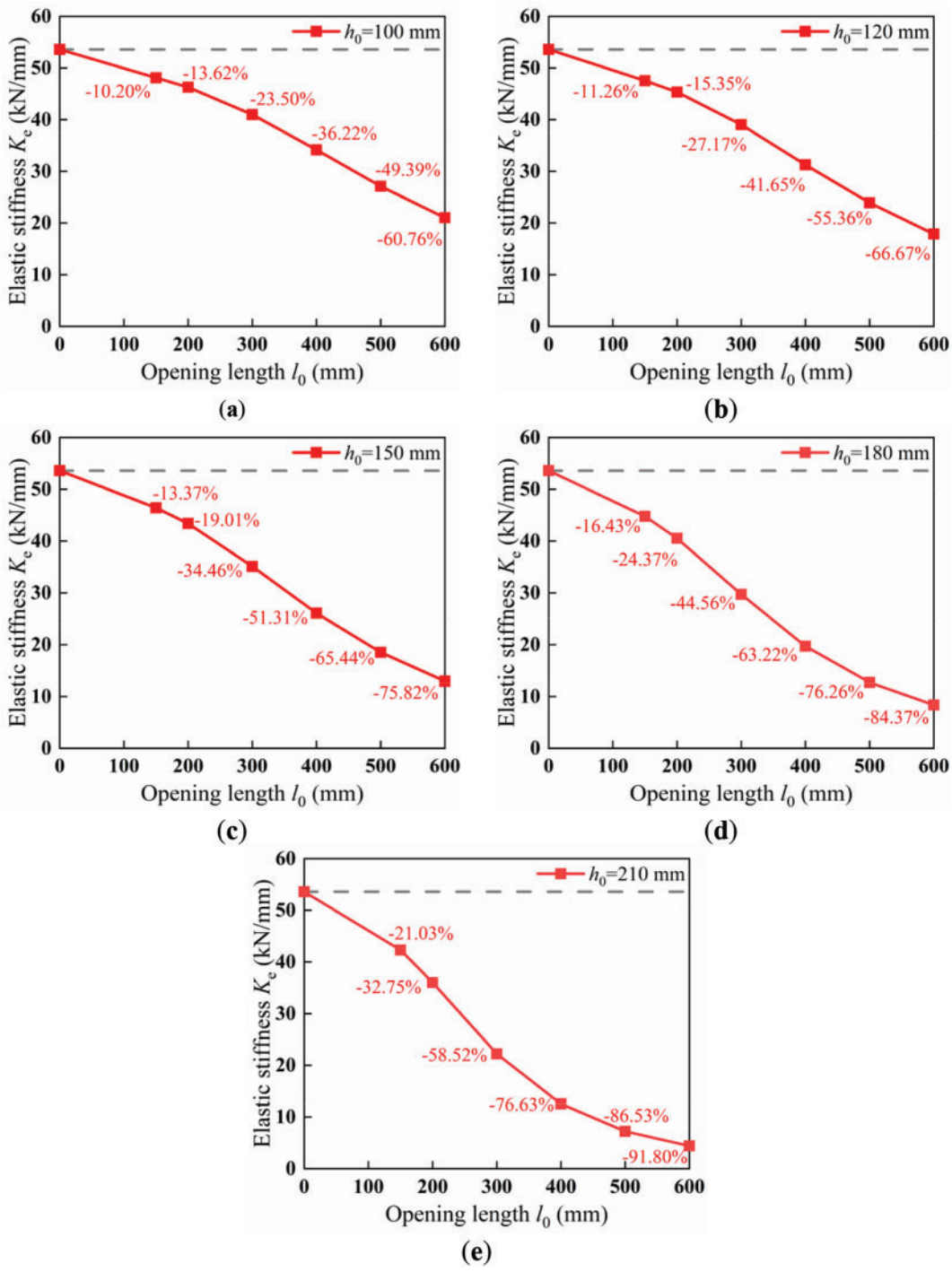

Figure 11: Elastic stiffness-opening line graph with different opening heights. (a) $h_0 = 100$ mm; (b) $h_0 = 120$ mm; (c) $h_0 = 150$ mm; (d) $h_0 = 180$ mm; (e) $h_0 = 210$ mm

As shown in Fig. 12, the ultimate load exhibited a monotonically decreasing trend with an increase in the opening length. The opening length is closely related to the weakening of the ultimate bearing capacity of the member. A larger opening length implies a smaller bearing capacity of the member.

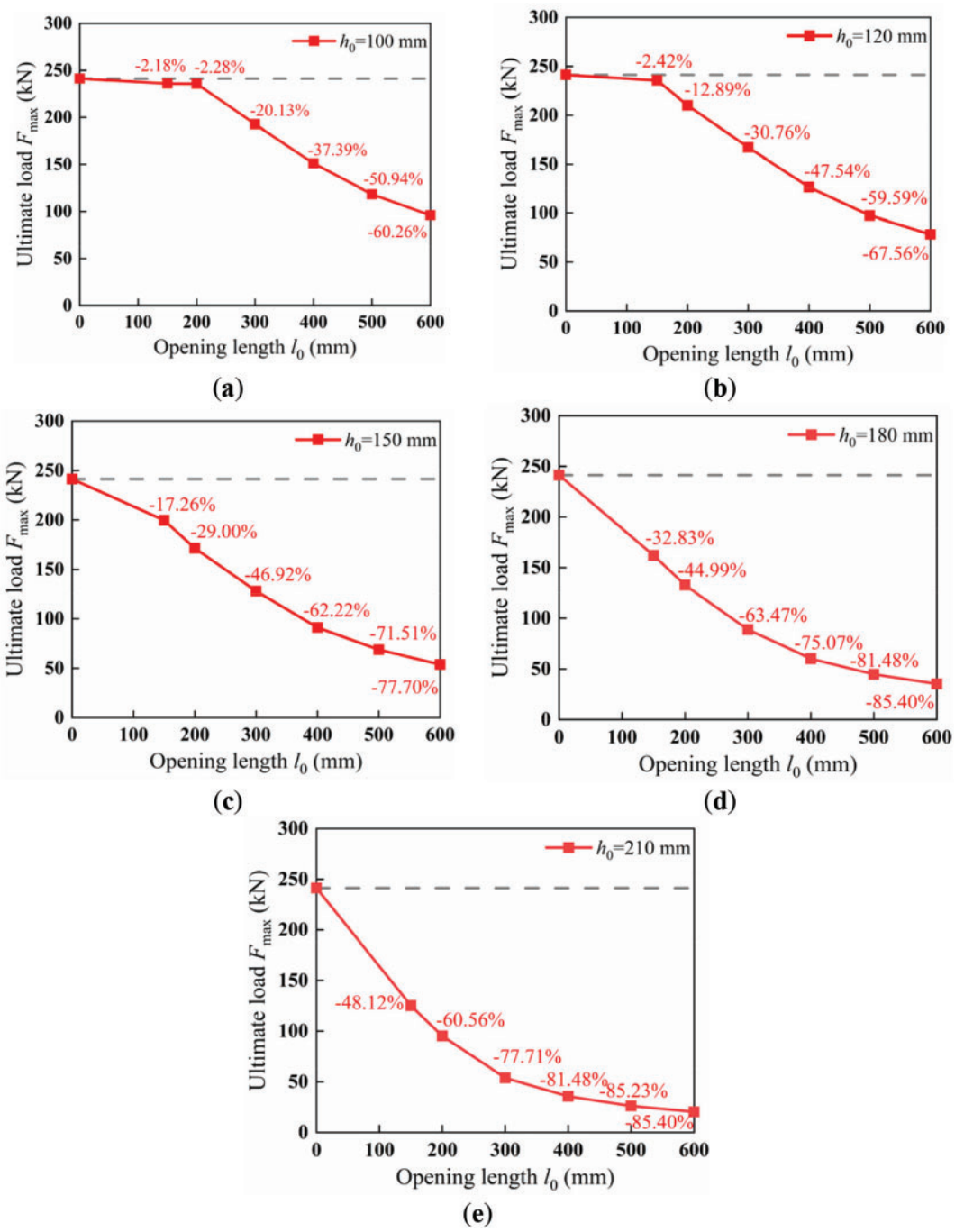

Figure 12: Ultimate load–opening length line graph with different opening heights. (a) $h_0 = 100$ mm; (b) $h_0 = 120$ mm; (c) $h_0 = 150$ mm; (d) $h_0 = 180$ mm; (e) $h_0 = 210$ mm

In Fig. 12a, the reduction percentage of the ultimate load of the model with a hole height of 100 mm and hole length of 600 mm is −60.26%, which indicates that even if the hole height is small, the ultimate load is greatly weakened when the hole length is large. In Fig. 12e, the reduction percentage of the ultimate load of the model with a hole height of 210 mm and hole length of 120 mm is −48.12%, which indicates that even if the hole length is small, the ultimate load is significantly weakened when the hole height is large.

3.3.2 Opening Height

As shown in Fig. 13a, the elastic stiffness decreases with an increasing opening height. For smaller opening lengths, the rate of decrease was relatively low; however, for larger opening lengths, the rate of decrease was more significant. The trend of the ultimate load–opening height breaking line in Fig. 11b was similar to that observed in Fig. 11a.

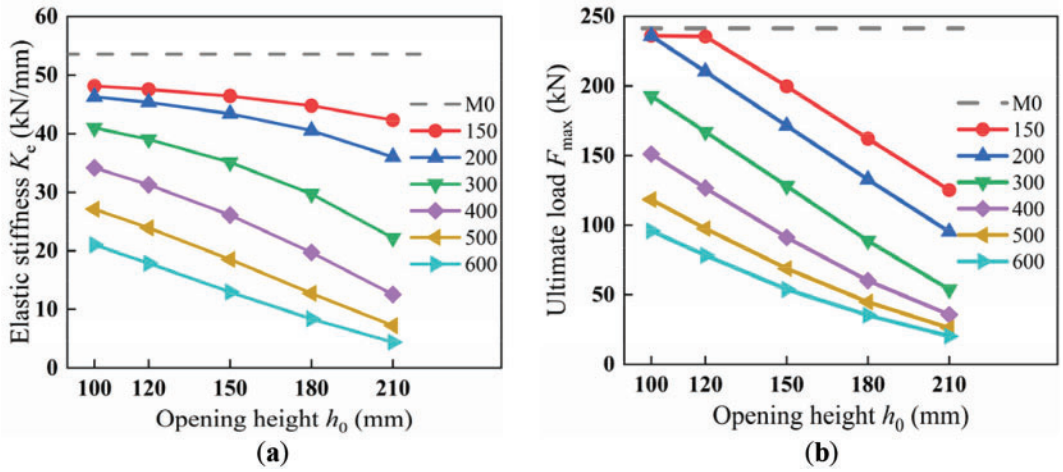

Figure 13: Elastic stiffness and ultimate load–opening height line diagram for models with different opening lengths. (a) Elastic stiffness; (b) Ultimate load

Comparing Figs. 12 and 13 shows that the degree of reduction of the increase of the opening rate caused by altering the opening length on the elastic stiffness of the member was slightly greater than the ultimate load.

3.4 Opening Distribution

To investigate the influence of changes in the opening distribution on the flexural performance of fixed-support open-web steel beams, the fixed hole height was set to 150 mm with an end distance of 100 mm. Considering four different opening rates (0.157, 0.210, 0.262, and 0.315) and three varying numbers of openings (3, 6, and 9), a uniform opening arrangement was adopted for each model. In this arrangement, the openings were evenly distributed between the holes. Fig. 14 presents a schematic illustrating the opening arrangement, encompassing a total of 12 models.

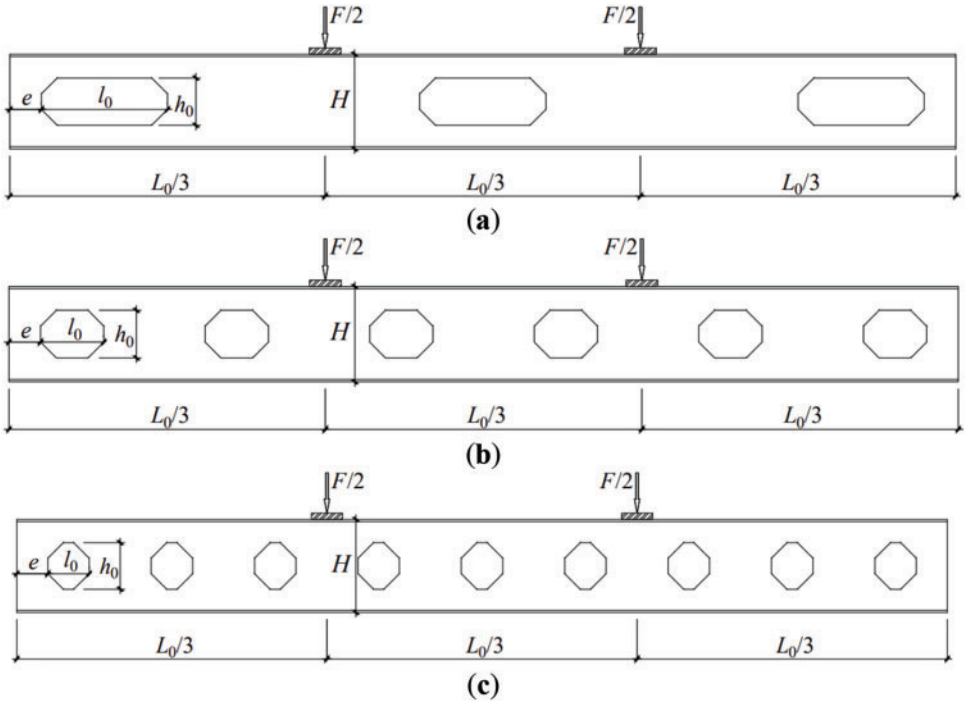

Figure 14: Opening diagram. (a) $n = 3$; (b) $n = 6$; (c) $n = 9$

3.4.1 Stress Nephogram

The failure process of the models with different opening rates was similar. Therefore, three models with $k = 0.210$ were used for the analysis. Fig. 15 shows the stress nephogram.

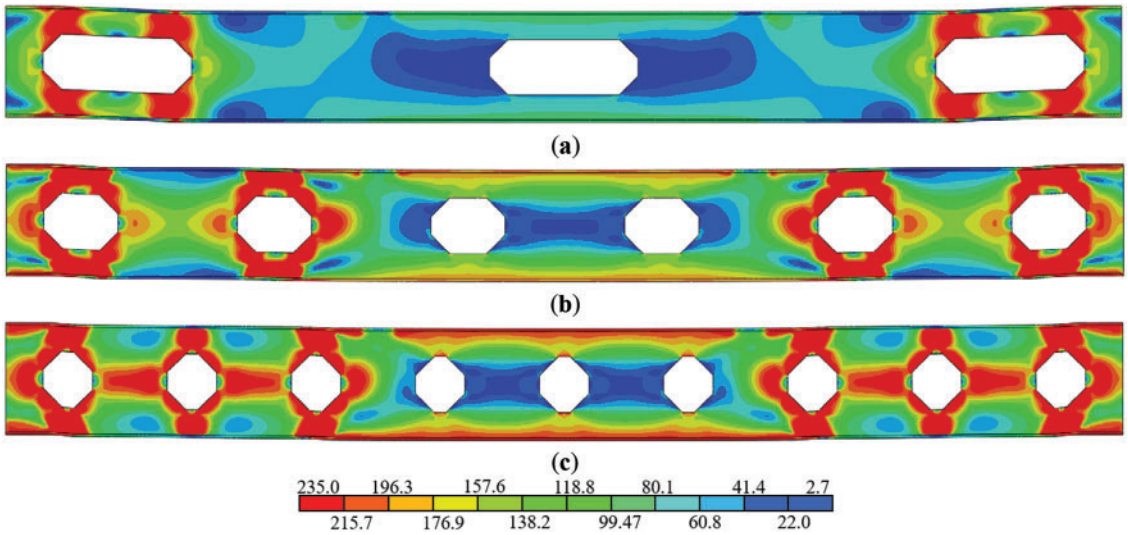

Figure 15: Stress nephogram (unit: MPa). (a) M-150-400-100-3; (b) M-150-200-100-6; (c) M-150-133.3-100-9

Fig. 15 illustrates that the high-stress region of an open-web steel beam is concentrated at the hole corner of the bending-shear section and that its failure mode is related to the distribution of the holes. When there are few holes, as shown in Fig. 15a, owing to the longer hole length, a "secondary shear moment" becomes apparent, and stress concentrates at the hole corner, forming four plastic hinges that lead to open-web failure. However, stress levels in pure bending sections located in the middle span remain low and fail to fully participate in force transmission. Conversely, when there are many holes (Fig. 15b,c), even with similar opening rates, single-hole lengths decrease with an increase in the number of holes, which results in uniform changes to the longitudinal section stiffness, which weakens the "secondary shear moment," thereby improving the flexural performance of open-web steel beams.

3.4.2 Elastic Stiffness and Ultimate Load

Fig. 16 illustrates the diagram of the elastic stiffness and ultimate load–opening number broken lines for different opening distribution models.

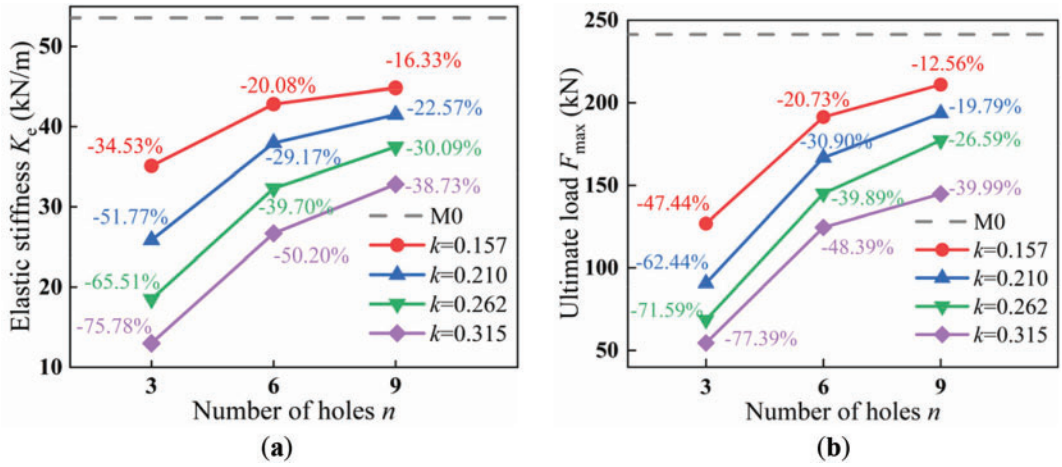

Figure 16: Elastic stiffness and ultimate load–number of holes line diagram with different opening distribution models. (a) Elastic stiffness; (b) Ultimate load

Fig. 16 shows that the number of openings exhibits a consistent influence on both the stiffness and bearing capacity of the member within an opening rate range of 0.157–0.315. Moreover, when the opening rate remained constant, there was a monotonic increase in both the elastic stiffness and ultimate load with an increasing number of openings. Notably, compared with the model with three openings, significant improvements in the elastic stiffness and bearing capacity were achieved by introducing six or nine openings into the model structure. For instance, at an opening rate of 0.262, the elastic stiffness values for models with 3, 6, and 9 openings were recorded as 18.48, 32.31, and 37.46 kN/m, respectively, whereas their corresponding ultimate loads were 68.58, 145.08, and 177.18 kN. Remarkably, the model with nine openings demonstrated an approximately one-fold improvement in both the stiffness and bearing capacity, compared with its counterpart with three openings, indicating that increasing the number of openings significantly improves both the elasticity and bearing capacity when maintaining a constant opening rate.

However, when the number of openings was 6, an increase in the number of openings did not significantly improve the flexural performance of the members. Thus, increasing the number of openings has a limited impact on the flexural performance. When there were 9 openings, both the

stiffness and bearing capacity reduction percentages of the member remained within 40%. These results indicate that evenly distributing these openings enables the estimation of the stiffnesses and bearing capacities of open-web steel beams by reducing the values from solid beams by approximately 40%. Furthermore, at an equal opening rate, increasing the number of evenly distributed openings can enhance the elastic stiffness and ultimate load-bearing capacity by approximately two times, compared with separate individual openings. Thus, it is recommended to distribute these openings as uniformly as possible to reduce the single-opening rates.

The broken line diagram in Fig. 17 illustrates the elastic stiffness and ultimate load–opening rate relationships for different opening distribution models.

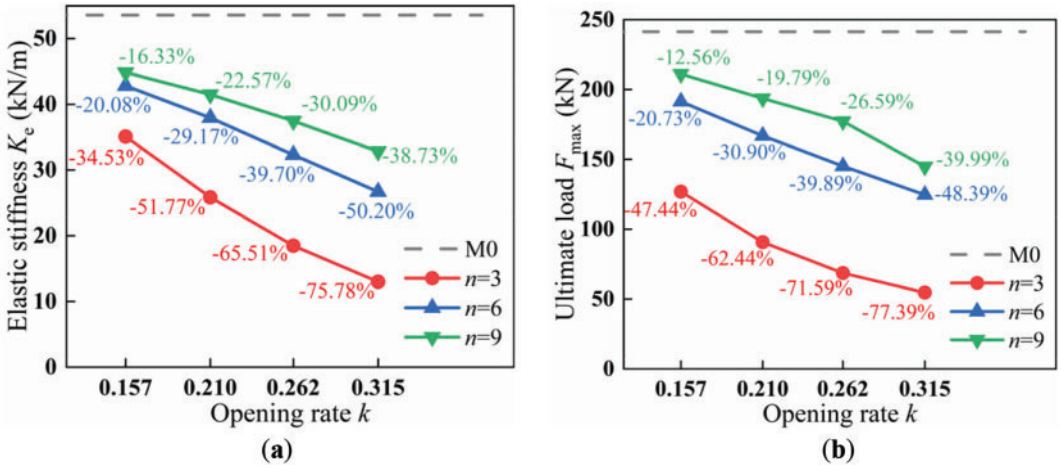

Figure 17: Elastic stiffness and ultimate load–opening rate line diagram with different opening distribution models. (a) Elastic stiffness; (b) Ultimate load

When the number of openings is constant, both the elastic stiffness and ultimate load of open-web steel beams exhibit a linear monotonic decrease with an increasing opening ratio. These findings align with the rule established in Section 3.3 that indicates its applicability, even in scenarios involving many openings.

4 Conclusion

This study investigated the influence of various parameters on the flexural performance of fixed open-web steel beams and proposed several design recommendations to guide the development and design of such beams. The following conclusions were drawn:

The position of the opening significantly affects the flexural performance of fixed open-web steel beams. When the end distance is less than 2.5 times the beam height (2.5 H), variations in this distance have a relatively stable impact on the flexural performance. To minimize the adverse effects of openings, it is recommended to position openings in the mid-span region. If an opening is required near the beam end, an end distance of approximately 1.75 H is recommended.

Increasing either the height or length of an opening leads to a reduction in the flexural performance of fixed open-web steel beams. This reduction becomes more notable as these dimensions of the opening increase. With identical hole height ratios, end distance ratios, and numbers of openings, the elastic stiffness and ultimate load exhibited linear monotonic declines with increasing opening rates.

The opening distribution plays a crucial role in determining the flexural performance of members. When maintaining equal opening rates, dispersing larger openings into smaller ones by reducing length-to-height ratios and increasing their number can enhance the stiffness and load-bearing capacity by approximately 100%, compared with using a single large opening. Therefore, it is advisable to distribute openings as evenly as possible while minimizing individual opening rates.

These findings provide valuable insights for the design and optimization of fixed open-web steel beams, emphasizing the importance of careful consideration of opening position, dimensions, distribution, and rate to achieve optimal structural performance.

Finally, this study acknowledges several limitations. For instance, the influence of residual stress was not considered during the modeling process. Future research could experimentally measure the residual stresses in open-web steel beams and incorporate them into numerical models to systematically investigate their impact on the mechanical performance of fixed open-web steel beams. Additionally, a review of the literature reveals a scarcity of experimental studies on fixed open-web steel beams, likely due to the challenges associated with achieving fixed supports in laboratory settings. Therefore, it is suggested to carry out experimental research on the mechanical behavior of fixed open-web steel beams.

Acknowledgement: The authors would like to express their sincere gratitude to all individuals and organizations that have contributed to the completion of this study. Firstly, we are deeply grateful to the following individuals for their invaluable assistance and support throughout the research process: Hongguang Xu, Zhengtao Xu, Huangcheng Lin. Secondly, we also thank the anonymous reviewers for their constructive comments and suggestions, which have greatly improved the quality of this paper. Finally, we would like to acknowledge any other contributions or assistance that have been essential to the completion of this study.

Funding Statement: The authors received no specific funding for this study.

Author Contributions: The authors confirm contribution to the paper as follows: study conception and design: Qingxing Feng; data collection: Qingxing Feng, Meizhong Qian, Chen Qu; analysis and interpretation of results: Qingxing Feng, Meizhong Qian, Chen Qu, Nihong Ye; draft manuscript preparation: Meizhong Qian, Chen Qu, Nihong Ye. All authors reviewed the results and approved the final version of the manuscript.

Availability of Data and Materials: The datasets generated and analyzed during the current study are available from the corresponding author on reasonable request.

Ethics Approval: Not applicable.

Conflicts of Interest: The authors declare no conflicts of interest to report regarding the present study.

References

1. Morkhade SG, Gupta LM. Behavior of castellated steel beams: state of the art review. Electron J Struct Eng. 2019;19(1):39–48. doi:10.56748/ejse.19234.
2. Wu Y, Wu D, Lin GD. A simplified calculation method for the bearing capacity of hexagon-hole castellated beam. J Harbin Inst Technol. 2009;41(2):5–8. doi:10.3321/j.issn:0367-6234.2009.02.002.

3. Morkhade SG, Gupta LM, Martins CH. Effect of web post width on strength capacity of steel beams with web openings: experimental and analytical investigation. Pract Period Struct Des Constr. 2022;27(2):1–9. doi:10.1061/(ASCE)SC.1943-5576.0000688.
4. Wang LF, Yang YF, Shi C. Load characteristics analysis of castellated beam based on ANSYS. J Chongqing Jianzhu Univ. 2004;26(2):72–5. doi:10.3969/j.issn.1674-4764.2004.02.016.
5. Al-Rifaie A, Al-Husainy AS, Al-Mansoori T, Shubbar A. Flexural impact resistance of steel beams with rectangular web openings. Case Stud Constr Mater. 2021;14:e00509. doi:10.1016/j.cscm.2021.e00509.
6. Song TW. Static behavior and design method of steel girders with large web openings [master's thesis]. Shanghai, China: Tongji University; 2007. (In Chinese).
7. Wang H. Research on the calculation method of rectangular hole castellated beam structure [master's thesis]. Dalian, China: Dalian University of Techonlogy; 2015. (In Chinese).
8. Liu ZN. Research on mechanical properties of rectangular hole castellated beams [master's thesis]. Dalian, China: Dalian University of Techonlogy; 2021.
9. Ponsorn P, Phuvoravan K. Efficiency of castellated and cellular beam utilization based on design guidelines. Pract Period Struct Des Constr. 2020;25(3):04020016. doi:10.1061/(ASCE)SC.1943-5576.0000497.
10. Zhu QH, Tong J, Tong GS. Effects of openings on steel beams and its design suggestions. Ind Constr. 2022;52(1):8. doi:10.13204/j.gyjzG21122107.
11. Xu HG. Theoretical and experimental study on hollow steel beam [master's thesis]. Hangzhou, China: Zhejiang University of Science and Technology; 2020. (In Chinese).
12. Xu HG, Feng QX, Duanmu XF, Xu ZS, Lin HC. Experimental study on influence of different chamfering forms on mechanical properties of hollow beams. J Zhejiang Univ Sci Technol. 2020;32(3):222–31. (In Chinese). [cited 2025 Jan 1]. Available from: https://xbbj.zust.edu.cn/html/202003009.html.
13. Xu HG, Feng QX, Duanmu XF, Xu ZS, Lin HC. Experimental study on the effect of openings on the bearing capacity and deflection of hollow beam. Build Struct. 2022;52(6):104–10. (In Chinese). doi:10.19701/j.jzjg.20200149.
14. Zou JH, Wei DM, Su YS, Li L. Reduced calculation and its experimental comparison for castellated beams. J South China Univ Technol Nat Sci Ed. 2005;33(1):47–51. doi:10.3321/j.issn:1000-565X.2005.01.010.
15. Zou JH. Experiment and analysis of the circular hole castellated beam [master's thesis]. Nanning, China: Guangxi University; 2003. (In Chinese).
16. Jia LG, Xu XX, Kang XZ. Finite element analysis of castellated beam maximum moment capacity. J Shenyang Jianzhu Univ Nat Sci. 2005;21(3):196–9. doi:10.3969/j.issn.2095-1922.2005.03.006.
17. Wang XT. Plastic capacity calculation of steel beams with web openings [master's thesis]. Kunming, China: Kunming University of Science and Technology; 2006. (In Chinese).
18. Luo L, Cai JN, Zhang HP. Improved calculation for normal stress in T-section of simply supported castellated steel beams. J Build Struct. 2016;37(S1):342–8. doi:10.14006/j.jzjgxb.2016.S1.048.
19. Hosseinpour M, Sharifi Y, Sharifi H. Neural network application for distortional buckling capacity assessment of castellated steel beams. Structures. 2020;27:1174–83. doi:10.1016/j.istruc.2020.07.027.
20. Maalek S. Shear deflections of tapered Timoshenko beams. Int J Mech Sci. 2004;46(5):783–805. doi:10.1016/j.ijmecsci.2004.05.003.
21. Li PF, Wang XM, Yuan Q, Guo M. Research on the deflection calculation of castellated beam based on area equivalent method. J Shijiazhuang Tiedao Univ Nat Sci Ed. 2011;24(3):7–11. doi:10.13319/j.cnki.sjztddxxbzrb.2011.03.022.
22. Zhou CY, Liu CJ. Calculation of flexural deflection for castellated beams. J Railw Sci Eng. 2007;4(1):72–6. (In Chinese). doi:10.19713/j.cnki.43-1423/u.2007.01.015.
23. Li QR. Experimental study on static performance of H-section column end plate connection of castellated beam [master's thesis]. Shenyang, China: Shenyang Jianzhu University; 2020. (In Chinese).

24. Huang BS, Huang TJ, Wang WC, Sang W. Calculation method of equivalent bending stiffness of castellated beams and analysis of its influence factors. J Build Struct. 2018;39(S2):121–7. doi:10.14006/j.jzjgxb.2018.S2.017.
25. Budi L, Sukamta, Partono W. Optimization analysis of size and distance of hexagonal hole in castellated steel beams. Procedia Eng. 2017;171:1092–9. doi:10.1016/j.proeng.2017.01.465.
26. Shamass R, Guarracino F. Numerical and analytical analyses of high-strength steel cellular beams: a discerning approach. J Constr Steel Res. 2020;166:105911. doi:10.1016/j.jcsr.2019.105911.
27. Morkhade SG, Lokhande RS, Gund UD, Divate AB, Deosarkar SS, Chavan MU. Structural behaviour of castellated steel beams with reinforced web openings. Asian J Civ Eng. 2020;21(6):1067–78. doi:10.1007/s42107-020-00262-y.
28. Deepha R, Jayalekshmi S. Finite element analysis on shear strength of a castellated beam with hexagonal web opening. IOP Conf Ser Mater Sci Eng. 2020;1006(1):012009. doi:10.1088/1757-899X/1006/1/012009.
29. Feng R, Liu J, Chen Z, Roy K, Chen B, Lim JBP. Numerical investigation and design rules for flexural capacities of H-section high-strength steel beams with and without web openings. Eng Struct. 2020;225:111278. doi:10.1016/j.engstruct.2020.111278.
30. Liang MD. Investigations on shear performance of splice plates connected castellated beams [master's thesis]. Jinan, China: Shandong University; 2020. (In Chinese).
31. Jiao YM. Research on the mechanical performance and bearing capacity calculation method of the castellated composite beam in the negative bending moment zone [master's thesis]. Shenyang, China: Shenyang Jianzhu University; 2021. (In Chinese).
32. Zhai YS. Study on bearing capacity and reinforcement method of prefabricated steel structure open-hole beams for apartments in Beijing Winter Olympic Village [master's thesis]. Fuxin, China: Liaoning Technical University; 2021. (In Chinese).
33. Huang W, Chen QG. Elasto-plastic behavior analysis of castellated beams. J Chongqing Univ Nat Sci Ed. 2006;29(4):87–90. (In Chinese). doi:10.3969/j.issn.1000-582X.2006.04.025.
34. Chen HR. Finite element analysis on hole radius of circular-web opening steel beams. J Qingdao Technol Univ. 2009;30(3):75–9. (In Chinese). doi:10.3969/j.issn.1673-4602.2009.03.013.
35. Su RQ, Xu JX, Dong WN. Numerical analysis of mechanical properties of castellated beam. J Gansu Sci. 2019;31(5):107–12. (In Chinese). doi:10.16468/j.cnki.issn1004-0366.2019.05.020.
36. Zheng ZA, Xia X, Ji W, Ye J, Wu J, Lin H. Experimental and numerical investigations on bending behavior of fixed open-web steel beams. Rev Int De Métodos Numéricos Para Cálculo Y Diseño En Ing. 2024;40(2):24. doi:10.23967/j.rimni.2024.05.007.